Biviscous horizontal simple shear zones of concentric arcs (Taylor–Couette flow) with incompressible Newtonian rheology

ARTICLE · JUNE 2015

Soumyajit Mukherjee

Indian Institute of Technology Bombay

Chapter 5
Biviscous horizontal simple shear zones of concentric arcs (Taylor–Couette flow) with incompressible Newtonian rheology

SOUMYAJIT MUKHERJEE[1] and RAKESH BISWAS[2]

[1] *Department of Earth Sciences, Indian Institute of Technology Bombay, Powai, Mumbai 400076, Maharashtra, India*
[2] *Geodata Processing and Interpretation Centre, Oil and Natural Gas Corporation Limited, Dehradun, India*

5.1 INTRODUCTION

> *Fluid caught between rotating cylinders has been intriguing physicists for over 300 years…*
>
> R.J. Donnelly (1991)

Ductile shear zones have so far been modeled mainly as zones of single lithology and with straight parallel and rigid boundaries (Ramsay 1980). Following this, thermal models of ductile shear zones were also provided (Fleitout and Froideavaux 1980). However, (i) natural shear zones can have curved boundaries in regional-scale, and (ii) may consist of more than one lithology. For example, crustal cross-sections of collisional orogens deduced from geophysical studies reveal shear zones with curved boundaries (Beaumont et al. 2001 and references therein). On the other hand, pronounced ductile shear segregates specific mineral assemblages for polymineralic rocks into zones with their interfaces parallel to the shear zone boundaries (Druguet et al. 2009). Layered shear zones have been reported/studied in granulite facies rocks (Ji et al. 1997), in models with ice (Wilson et al. 2003), from collisional terrains (Mukherjee and Koyi 2010), and in granular materials (Börzsönyi et al. 2009), besides most common cases of micaceous minerals alternating with quartzofeldspathic minerals in mylonites (Lister and Snoke 1984). Those two natural cases (i) and (ii) have recently been modeled individually (Mukherjee and Biswas 2014; Mulchrone and Mukherjee, in press) to deduce velocity profiles and shear senses. This work considers the two cases together to deduce and interpret velocity profiles of biviscous curved ductile simple shear zones. We do not address here shear zone related folds (see Mukherjee et al. this volume, Chapter 12).

5.2 THE MODEL

We use the Taylor–Couette flow model (Taylor 1923) to explain the kinematics of biviscous curved shear zone, as follows. Consider a ductile shear zone with concentric circular boundaries of radii R_1 and R_2 ($R_1 > R_2$) with two immiscible incompressible Newtonian viscous fluids within: an outer layer of fluid A with a viscosity μ_a, and an inner fluid layer B with a viscosity μ_b ($\mu_a > \mu_b$). Their interface is a circle of radius R_b. The inner boundary rotates clockwise with an angular velocity ω and the outer boundary remains static. Such flow in fluid mechanics has been known as Taylor–Couette flow/circular Couette shear, etc. for a long time (Donnelly, 1991), both for rotation of two boundaries and one of the boundaries, and for single and two fluids (Schulz et al. 2003). Even if one considers the two fluids (in geology, "ductile lithologies") were mixed, upon circular shear they segregate with lighter fluid near the core and the denser fluid near the periphery (Baier 1999; Vedantam et al. 2006). Taylor–Couette flow has already been classified in fluid mechanics into three types: (i) homogeneous dispersion, (ii) banded dispersion, and (iii) segregated/stratified flow. We discuss here a kind of stratified flow.

The velocity distributions in both the layers obey the velocity equation:

$$v_\theta = (C_1/2)r + C_2(1/r) \tag{1}$$

(from eqn 15.38 of Williams and Elder 1989)

$$\text{Velocity equation for fluid A}: v_\theta^a = \left(C_1^a/2\right)r + C_2^a(1/r) \tag{2}$$

$$\text{That for fluid B is}: v_\theta^b = \left(C_1^a/2\right)r + C_2^b(1/r) \tag{3}$$

Here v_θ is azimuthal velocity; θ is meridional angle (Fig. 5.1a); C_1^a, C_2^a, C_1^b, and C_2^b are integration constants.

$$\text{At } r = R_1, v_\theta^a = 0 \tag{4}$$

And at

$$r = R_2, v_\theta^b = R_2\omega \tag{5}$$

Ductile Shear Zones: From Micro- to Macro-scales, First Edition. Edited by Soumyajit Mukherjee and Kieran F. Mulchrone.

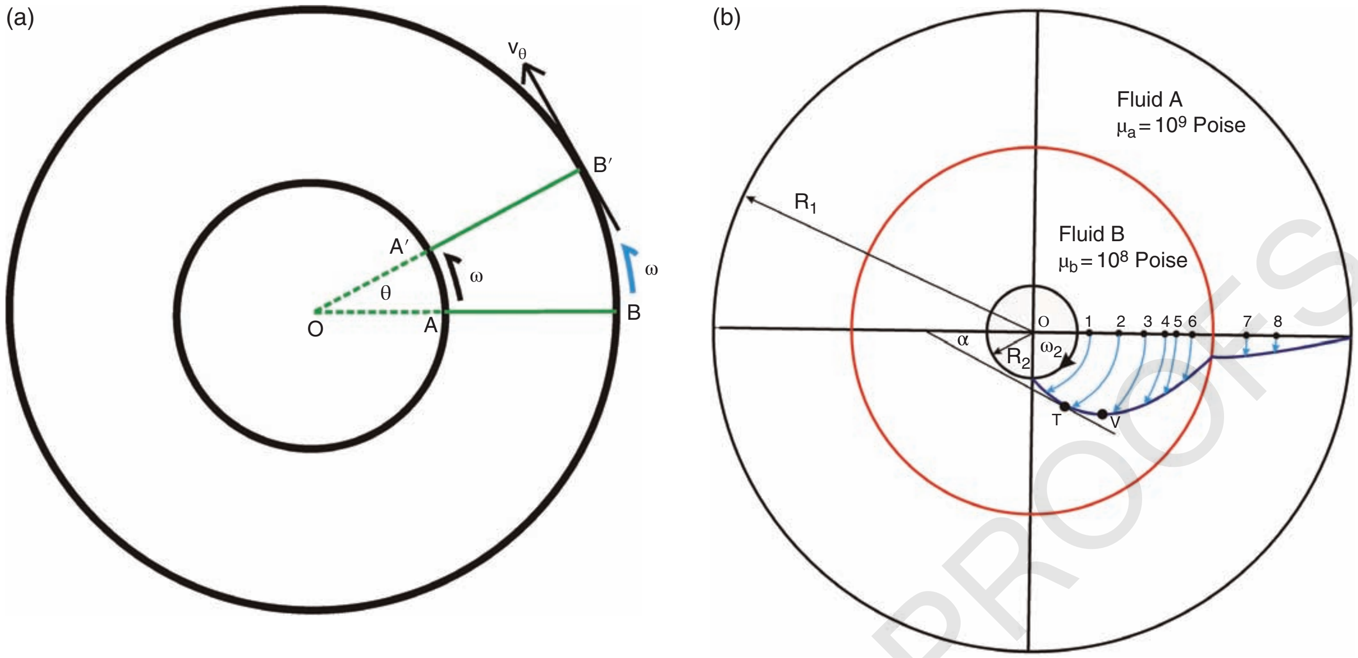

Fig. 5.1. (a) Angular velocity ω acts on the two concentric circular boundaries of a curved horizontal shear zone. A marker AB turns A′B′. The meridional angle (θ) and the azimuthal velocity (v_θ) are shown. Source: Mukherjee & Biswas, 2014. Reproduced with permission from Springer Science + Business Media. (b) Velocity profiles for Taylor–Couette flow with two Newtonian fluids "A" and "B" within two concentric circular boundaries. The red circle marks the interface between the two fluids. The inner boundary rotates clockwise. The outer boundary is static. Here R_1 = 100 cm., R_2 = 50 cm, ω = 2° hr^{-1}, μ_a = 10^9 Poise and μ_b = 10^8 Poise.

At the interface, $r = R_b$, the two additional conditions are as follows. (i) The two fluids stick together:

$$v_\theta^a = v_\theta^b \tag{6}$$

(ii) The momentum transfer through the interface is continuous:

$$\tau_{r\theta}^a = \tau_{r\theta}^b \text{ at } r = R_b \tag{7}$$

Or,

$$\mu_a r \frac{d}{dr}\left(\frac{v_\theta^a}{r}\right) = \mu_b r \frac{d}{dr}\left(\frac{v_\theta^b}{r}\right) \tag{8}$$

Using Equations 2 to 8 and after doing some algebra, the velocity equations for fluids A and B are:

$$v_\theta^a = \left\{\left(\mu_b \omega R_b^2 R_2^2 R_1^2\right) / \left[\mu_b\left(R_1^2R_2^2 - R_b^2R_2^2\right) - \mu_a\left(R_1^2R_2^2 - R_b^2R_1^2\right)\right]\right\} \times \left(\frac{1}{r} - \frac{r}{R_1^2}\right) \tag{9}$$

$$v_\theta^b = \omega r + \left\{\left(\mu_a \omega R_b^2 R_2^2 R_1^2\right) / \left[\mu_b\left(R_1^2R_2^2 - R_b^2R_2^2\right) - \mu_a\left(R_1^2R_2^2 - R_b^2R_1^2\right)\right]\right\} \times \left(\frac{1}{r} - \frac{r}{R_2^2}\right) \tag{10}$$

Notice that the velocity equations depend on the viscosity of both the fluids. Starting from line OI, velocity profiles developed in the two fluids are shown in Fig. 5.1b. Flow paths of both the fluids are segments of circles that are concentric with the circular boundaries of the shear zone. Angular shear at some particular moment can be measured at any point on the profile by drawing a tangent at that point and finding the angle between that tangent and the line OI (Fig. 5.1b). The point of highest curvature on the velocity profile is shown as 'V' in Fig. 1b, which is also the point of highest speed induced by ductile shear of the curved inner boundary. Reverse ductile shear senses develop simultaneously across point 'V'. In detail: from the outer boundary of the circular shear zone up to point 'V', a shear sense same as that produced by the rotating inner boundary is produced. From 'V' up to the inner boundary, an opposite ductile shear sense develops. The point of intersection between the velocity profile and the line OI, point 'I', is called the "neutral point". It is the unique static point inside the shear zone. A circle concentric with the shear zone boundaries and passing through the neutral point is called the "neutral curve" (Mukherjee and Biswas 2014). Material points on the neutral curve remain stationary during ductile shear. In the present case, the neutral curve coincides with the static outer boundary of the shear zone. Note that the term "neutral curve" has been used here in a different context than that used by Fossen and Rykkelid (1992), Peng and Zhu (2010), and Ovchinnikova (2012). Had there been rotation of the outer curved boundary of the shear zone in a direction opposite to that of the inner boundary (that is, anticlockwise), the neutral point would have plotted inside the shear zone. Note that we can at best decipher relative shear movements in shear zones, and not the absolute movements of its boundaries. Therefore, locating neutral point in real shear zones seems not possible even though it is discussed here. Taylor–Couette flow apparatus has been in use in structural geological analogue models to simulate high-strain ductile shear (e.g. Bons and Jessell 1999).

Shear strain (tanα) at any point 'T' on the profile (Fig. 5.1b) can be obtained from the angle α between the tangent at 'T' on the profile and the line AI. Figure 5.2 shows how shear strain varies inside the model shear zone measured for eight points with initial positions '1' to '8' shown in Fig. 5.1b. Shear strain is minimum at 'V' and increases away from it in both directions. Higher shear strain attains within Fluid B- at few locations than in Fluid A layer: compare the plots in Fig. 5.2 for points '7' and '8' with points '1', '2', '4', '5', and '6'.

Five circular markers of equal radius before deformation (Fig. 5.3), considered in both the fluid layers on ductile shear, become irregular shaped, indicating their non-homogeneous deformation. Figure 5.4 shows the temporal evolution of aspect ratios of these markers at four instances. In general, aspect ratios increase temporally. It can also decrease since points 'y' and 'z' (inset in Fig. 5.3), that were increasing distance between them during deformation, can also start decreasing. This can be understood from the green dots showing evolution of marker 'd' in Fig. 5.4. The inset in Fig. 5.4 defines the aspect ratio tentatively from irregular objects. Marker 'c' was positioned deliberately partly in one fluid layer and partly in the other. Fluid 'B' undergoes more shear than that of fluid 'A', as can be visually appreciated more from marker 'c'. The reasons are, first: only the (inner) boundary of the curved zone shears. Second, fluid B is less viscous than fluid A. This is also corroborated from shear strains within these layers (Fig. 5.2). Biviscous Taylor–Couette flows may develop instability at the contact between the two fluid layers (Gelfgat et al. 2004). This manifest as warping of the interface. The present study did not consider development of such an instability. Andereck et al. (1986) pointed out that Taylor–Couette flow kinematics depends on aspect ratio and radius ratio of the region where the fluid is kept, and on the Reynold's number of the fluid. Taylor–Couette flow has been studied in fluid mechanics for a single rotating cylinder and for rotation of both cylinders (White 2005). Layered Taylor–Couette flow of non-Newtonian fluids for eccentric/non-axisymmetric cylinder are already available in fluid mechanics, such as Escudier et al. (2002). We are working to adopt them in ductile shear zone studies in structural geology.

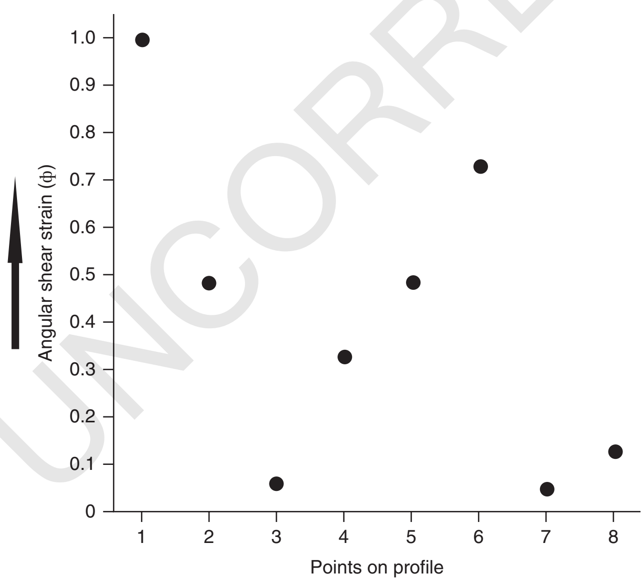

Fig. 5.2. Magnitudes of shear strain variation in biviscous shear zone, detailed in the caption of Fig. 5.1, at one particular instant. Locations of points "1" to "8" on the marker before shear are shown in Fig. 5.1b.

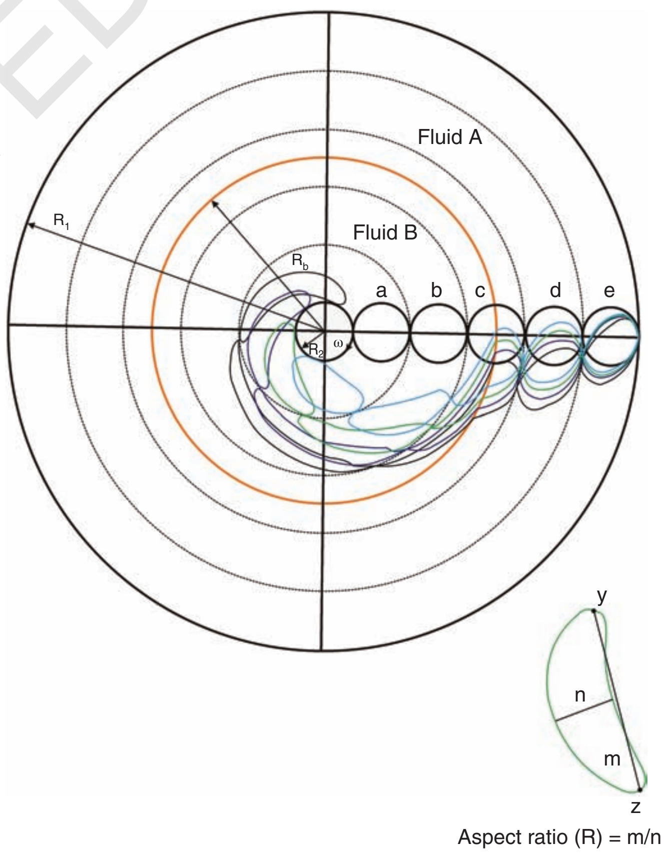

Fig. 5.3. Five circular markers, "a" to "e", inside a concentric circular shear zone. Caption of Fig. 5.1 presents detail of the shear zone. Sky blue markers: markers after 60 hr, green markers: after 90 hr, deep blue markers: after 120 hr, and black markers: after 150 hr. $\omega = 2° \text{ hr}^{-1}$.

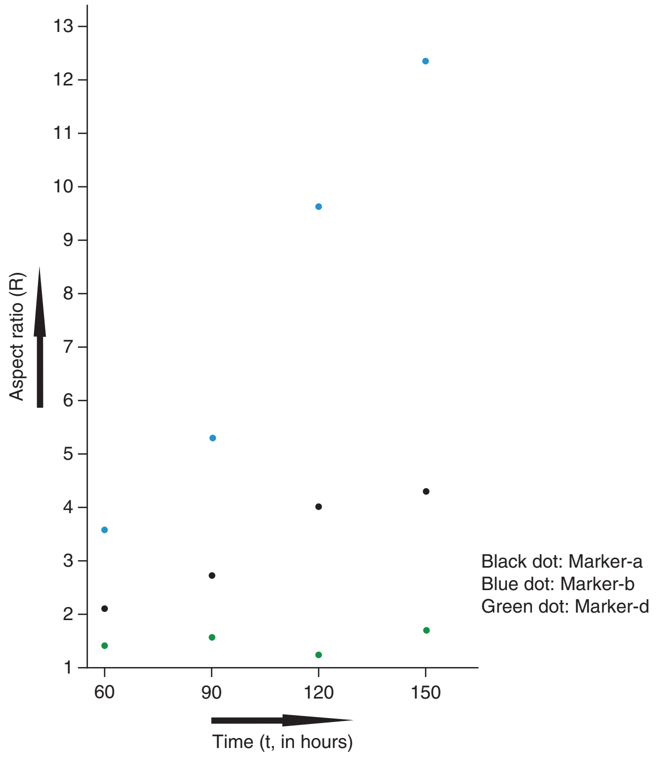

Fig. 5.4. Temporal variation of aspect ratios of three markers, "a", "b", and "d".

ACKNOWLEDGMENTS

Department of Science and Technology's (New Delhi) grant number: SR/FTP/ES-117/2009 supported SM. RB received IIT Bombay's fellowship. Gretchen Baier (The Dow Chemical Company) and Christoph Schrank (Queensland University of Technology) are thanked for providing internal reviews.

REFERENCES

Andereck CD, Liu SS, Swinney HL. 1986. Flow regimes in a circular-Couette system with independently rotating cylinders. Journal of Fluid Mechanics 164, 155–183.

Baier G. 1999. Liquid-liquid extraction based on a new flow pattern: Two fluid Taylor Couette flow. PhD thesis. University of Wisconsin – Madison. pp. 1–231.

Baier G, Graham MD. 2000. Two-fluid Taylor–Couette flow with countercurrent axial flow: Linear theory for immiscible liquids between corotating cylinders. Physics of Fluids 12, 294–303.

Beaumont C, Jamieson RA, Nguyen MH, Lee B. 2001. Himalayan tectonics explained by extrusion of a low-viscosity crustal channel coupled to focused surface denudation. Nature 414:738–742.

Bons PD, Jessell MW, 1999. Micro-shear zones in experimentally deformed octachloropropane. Journal of Structural Geology 21, 323–334.

Börzsönyi T, Unger T, Szabó1 B. 2009. Shear zone refraction and deflection in layered granular materials. Physical Review E 80, 060302(R).

Donnelly RJ. 1991. Taylor Couette flow: The early days. Physics Today 32, 36–39.

Druguet E, Alsop GI, Carreras J. 2009. Coeval brittle and ductile structures associated with extreme deformation partitioning in a multilayer sequence. Journal of Structural Geology, 31, 498–511.

Escudier MP, Oliveira PJ, Pinho FT (2002) Fully developed laminar flow of purely viscous non-Newtonian liquid through annuli, including the effects of eccentricity and inner cylinder rotation. International Journal of Heat and Fluid Flow 23, 52–73.

Fleitout L, Froideavaux C. 1980. Thermal and mechanical evolution of shear zones. Journal of Structural Geology, 2, 159–164.

Fossen, H., Rykkelid, E. The interaction between oblique and layer-parallel shear in high-strain zones: Observations and experiments. Tectonophysics 207, 331–343.

Gelfgat AY, Yarin A, Bar-Yoseph PZ, Graham MD, Bai G. 2004. Numerical modeling of two-fluid Taylor–Couette flow with deformable capillary liquid–liquid interface. Physics of Fluids 16, 4066–4047.

Ji S, Long C, Martignole J, Salisbury M. 1997. Seismic reflectivity of a finely layered, granulite-facies ductile shear zone in the southern Grenville Province (Quebec). Tectonophysics 279, 113–133.

Lister GS, Snoke AW. 1984. S-C Mylonites. Journal of Structural Geology 6, 617–638.

Masuda T, Mizuno N, Kobayashi M, Nam TN. 1995. Stress and strain estimates for Newtonian and non-Newtonian materials in a rotating shear zone. Journal of Structural Geology 17, 451–454.

Mukherjee S, Biswas R. 2014. Kinematics of horizontal simple shear zones of concentric arcs (Taylor–Couette flow) with incompressible Newtonian rheology. International Journal of Earth Sciences 103, 597–602.

Mukherjee S, Koyi HA, 2010. Higher Himalayan Shear Zone, Sutlej section: structural geology and extrusion mechanism by various combinations of simple shear, pure shear and channel flow in shifting modes. International Journal of Earth Sciences 99, 1267–1303.

Mukherjee S, Punekar JN, Mahadani T, Mukherjee R. this volume. Intrafolial folds- review & examples from the western Indian Higher Himalaya. In Ductile Shear Zones: from micro- to macro-scales, edited by S. Mukherjee and K.F. Mulchrone, this book.

Mulchrone KF, Mukherjee S. in press. Shear senses and viscous dissipation of layered ductile simple shear zones. Pure and Applied Geophysics, doi: 10.1007/s00024-015-1035-8.

Ovchinnikova SN. 2012. Oscillatory instability of the Couette flow between the two unidirectionally rotating cylinders. Fluid Dynamics 47, 454–464.

Peng J, Zhu K-Q. 2010. Linear instability of two-fluid Taylor–Couette flow in the presence of surfactant. Journal of Fluid Mechanics 651, 357–385.

Ramsay JG, 1980. Shear zone geometry: a review. Journal of Structural Geology 334 83–99.

Wilson CJL, Russell-Head D.S., Sim HM. 2003. The application of an automated fabric analyzer system to the textural evolution of folded ice layers in shear zones. Annals of Glaciology 37, 7–17.

Sathe MJ, Deshmukh SS, Joshi JB, Koganti SB, 2010. Computational fluid dynamics simulation and experimental investigation: study of two-phase liquid–liquid flow in a vertical Taylor–Couette contactor. Industrial & Engineering Chemistry Research 49, 14–28.

Schulz A, Pfister G, Tavener SJ, 2003. The effect of outer cylinder rotation on Taylor–Couette flow at small aspect ratio. Physics of Fluids 15, 417–425.

Taylor GI, 1923. Stability of a viscous liquid contained between rotating cylinders. Philosophical Transactions of the Royal Society of London A 223, 289–343.

Vedantam S, Joshi JB, Koganti SB, 2006. Three-dimensional CFD simulation of stratified two-fluid Taylor–Couette flow. The Canadian Journal of Chemical Engineering 84, 279–288.

Williams J, Elder SA, 1989. Fluid Physics for Oceanographers and Physicists. Pergamon Press, Oxford, pp. 253–255.

White FM. 2005. Viscous Fluid Flow. Tata McGraw-Hill Education, New York.

PART II

Examples from Regional Aspects